

# A systematic study of neutron magic nuclei with $N = 8, 20, 28, 50, 82$ , and 126 in the relativistic mean field theory

L. S. Meng,<sup>1,2</sup> H. Toki,<sup>1</sup> and J. Meng<sup>2</sup>

<sup>1</sup>Research Center for Nuclear Physics (RCNP), Osaka University, Ibaraki, Osaka 567-0047, Japan

<sup>2</sup>School of Physics, Peking University, Beijing 100871, People's Republic of China

We perform a systematic study of all the traditional neutron magic isotopic chains:  $N = 8, 20, 28, 50, 82$ , and 126, from the neutron drip line to the proton drip line. We adopt the deformed relativistic mean field (RMF) theory as our framework and treat pairing correlations by a simple BCS method with a zero-range force. Remarkable agreement with available experimental data is obtained for the binding energies, the two- and one-proton separation energies, and the nuclear charge radii. The calculated nuclear deformations are compared with the available experimental data and the predictions of the FRDM model. We discuss, in particular, the appearance of sub-shell magic nuclei by observing irregular behavior in the two- and one-proton separation energies.

## I. INTRODUCTION

"Magic number" is a very important concept in many subjects of physics, such as atomic physics, nuclear physics and micro cluster physics. In nuclear physics, nuclei with magic numbers have been hot topics of nuclear research since the beginning of this subject [1, 2]. In recent experiments with radioactive nuclear beams (RNB), disappearance of traditional magic numbers and appearance of new magic numbers are observed in nuclei with exotic isospin ratios. Furthermore, nuclei with magic neutron numbers in the neutron-rich region are of special interest for the study of astrophysical r-process [3].

The unusual stability of nuclei with neutron (proton) numbers 2, 8, 20, 28, 50, 82, and 126, commonly referred to as "magic numbers", was traditionally explained in the nonrelativistic shell model approximately by the 3D harmonic oscillator central potential together with a very strong spin-orbit interaction introduced by hand [1, 2, 4, 5, 6]. On the other hand, in the models within the relativistic framework, say the relativistic mean field (RMF) theory [7, 8, 9, 10, 11], the strong spin-orbit interaction appears naturally as the interplay between the strong scalar and vector potentials, which are necessary for the production of the saturation property of nuclear matter. Due to the proper setting of the scalar and the vector potentials the shell structure is obtained without any additional parameters for the spin-orbit splittings. In this paper, we would like to use the relativistic mean field (RMF) theory to study all the  $N = 8; 20; 28; 50; 82$ , and 126 isotopic chains.

Recently, it is argued that the magic numbers are of a localized feature, i.e., in nuclei with exotic isospin ratios the classical magic numbers do not necessarily hold and new magic numbers may appear. There have been several experimental evidences supporting such a belief, as the lately reported  $N = 82$  shell quenching [12] and the appearance of a new neutron magic number  $N = 16$  in the neutron-rich light nuclei [13]. Such a localized feature of magic numbers are also claimed important for various nuclear astrophysical problems [14]. The disappearance or quenching of nuclear magicity near both neutron and

proton drip lines have been discussed quite a lot in various nuclear models, such as the infinite nuclear matter (INM) model [15], the extended Bethe-Wiezsäcker mass formula [16], the antisymmetrized molecular dynamics (AMD) [17], the Hartree-Fock method [18], and the relativistic mean field (RMF) [19, 20] theory. In the relativistic mean field models, while the  $Z = 8, 20, 28, 50, 82$ , and 126 isotopic chains have been discussed a lot, a systematic study of all the nuclei with neutron magic numbers is still missing.

The appearance and disappearance of the magic number effect are intimately related with the spin-orbit interaction and the onset of deformation. In this sense, a systematic study of nuclei in various mass regions in terms of the relativistic mean field theory is suited, since the spin-orbit interaction arises naturally in relation with the saturation property. Hence, we are able to provide the change of the spin-orbit splittings with the proton and neutron numbers. As for the deformation, nuclei with some magic numbers are not easy to acquire deformation, since the onset of deformation does not utilize the energy gain coming from the large shellgaps. At the same time, due to this reason it is easier to find the appearance of the sub-magic effects for nuclei with either the proton number or the neutron number being some magic numbers.

In the present work, we would like to make a systematic study of neutron magic nuclei from the neutron drip line to the proton drip line in terms of the deformed relativistic mean field theory. The pairing correlations are also very important to make the nucleus tend to be spherical. We take the recently proposed method of using the zero-range force for the pairing correlations in order to pick up the resonance states in the continuum, when the nucleus approaches the neutron threshold [21]. We perform the constrained RMF calculations in order to find all the energy minima as a function of the nuclear deformation. In this paper, we stay our calculations at the mean field level and hence anticipate that we may miss the onset of small deformation in this framework for the case when the deformation effect is not dominant. Hence, the purpose of this paper is to make a systematic study

of the neutron magic isotonic nuclei in the mean field framework and compare with the available experimental data in the global sense and with other more sophisticated theoretical frameworks for particular nuclei. We mention that even at the mean field level, there appear many nuclei with deformation for the proton magic nuclei [20].

This paper is organized as follows. We provide a short summary of the deformed RMF+BCS method in Sec. II. In Sec. III-V, we present results of our calculations including the binding energies, the two- and one-proton separation energies, the nuclear radii, and the nuclear deformations. With these quantities, we also discuss the magicity of these six neutron magic number isotonic nuclei,  $N = 8, 20, 28, 50, 82$ , and  $126$ . The whole work is summarized in Sec. VI.

## II. THEORETICAL FRAMEWORK

In the present work, the recently proposed deformed RMF+BCS method with a zero-range  $\delta$ -force in the pairing channel is adopted [21]. The zero-range  $\delta$ -force has proved to be very successful to take into account the continuum effect by picking up resonance states both in relativistic and nonrelativistic self-consistent mean field models [21, 22, 23, 24, 25, 26]. In the mean field part, the TM A parameter set is used [27]. The RMF calculations have been carried out using the model Lagrangian density with nonlinear terms for both and  $\pi$  mesons as described in detail in Refs. [21, 27], which is given by

$$\begin{aligned} L = & (i \partial \cdot M) \\ & + \frac{1}{2} \partial \cdot \partial - \frac{1}{2} m^2 \cdot \partial^2 - \frac{1}{3} g_2^3 - \frac{1}{4} g_3^4 + g \\ & + \frac{1}{4} \partial^2 + \frac{1}{2} m^2 \cdot \partial^2 + \frac{1}{4} g_4^2 (\partial^2)^2 - g_1^2 \cdot \partial^2 \\ & + \frac{1}{4} R^a \cdot R^a + \frac{1}{2} m^2 \cdot a^a \cdot a^a - g \cdot a^a \cdot a^a \\ & + \frac{1}{4} F^a \cdot F^a - e \cdot \frac{1}{2} \overline{A}^3 \cdot A^a; \end{aligned} \quad (1)$$

where all symbols have their usual meanings. The corresponding Dirac equation for nucleons and Klein-Gordon equations for mesons obtained with the mean field approximation are solved by the expansion method in the widely used axially deformed harmonic oscillator basis [21, 28]. The number of shells used for expansion is chosen as  $N_f = N_b = 20$ . More shells have been tested for convergence considerations. The quadrupole constrained calculations have been performed for all the nuclei considered here in order to determine their ground-state deformations and obtain potential energy surfaces (PESs) [21, 29]. For nuclei with odd number of nucleons, a simple blocking method without breaking the time reversal symmetry is adopted [5, 30]. The pairing strength  $V_0$  is taken the same for both protons and neutrons, but optimized for different regions by fitting the experimental two- and one-proton separation energies, more specifically, for the  $N = 8, 20, 28, 50$  isotonic chains,  $V_0 = 344.1 \text{ MeV fm}^3$ ; for the  $N = 82, 126$  isotonic chains,  $V_0 = 310 \text{ MeV fm}^3$ .

## III. BINDING ENERGIES

The nuclear binding energy is one of the most basic properties of nuclei. Although the two- and one-proton separation energies are more useful for the purpose of identifying the shell structure, the total binding energies of nuclei can also show some important features of a theoretical model, such as the reliability of extrapolation to the unknown areas. In Fig. 1, we plot the total binding energies for all the six isotonic chains with neutron number  $N = 8, 20, 28, 50, 82$  and  $126$  as a function of the proton number  $Z$ . Remarkable agreement with the experimental data [31] is clearly seen. For the  $N = 8$  isotonic chain, the experimental trend is reproduced quite well. The only small discrepancy is that the calculated results are somewhat systematically larger than the experimental data. Anyway, it is remarkable that a mean field model can reproduce such light nuclei so well without fitting the parameters particularly for this region. For the  $N = 126$  isotonic chain, theory agrees well with experiment around  $^{208}\text{Pb}$ . The results for nuclei with more protons begin to deviate from the experimental data, i.e. the calculated results are larger than the experimental data. The use of other parameter sets, NL3 [32] and NL-Z2 [33], does not change this conclusion.

## IV. TWO- AND ONE-PROTON SEPARATION ENERGIES

The two- and one-proton separation energies

$$S_{2p}(N;Z) = B(N;Z) - B(N-2;Z); \quad (2)$$

$$S_p(N;Z) = B(N;Z) - B(N-1;Z); \quad (3)$$

where  $B(N;Z)$  is the binding energy of the nucleus with neutron number  $N$  and proton number  $Z$ , are quite important and sensitive quantities to describe nuclei and the corresponding shell closures. In Fig. 2, we plot the two- and one-proton separation energies for all the  $N = 8, 20, 28, 50, 82$ , and  $126$  isotonic chains as a function of the proton number  $Z$ . A larger drop than its neighboring counterparts in these curves is usually interpreted as a (sub)shell closure, and the corresponding nucleon number is called "(sub)magic number". In the present work, we mainly adopt such a notion to discuss shell closures.

In Fig. 2, we show the calculated results on the two- and one-proton separation energies of all the neutron magic number nuclei in the deformed RMF+BCS method with the TM A parameter set and compare with available experimental data [31]. We should mention that some experimental data from Ref. [31] are obtained from "distant connection" and that we do not make any distinction between real experimental data and extrapolated data. From Fig. 2, it is quite clear that the theoretical calculations agree remarkably well with the experimental data

in the whole region from mass number 11 ( $^{11}\text{Li}$ ) to mass number 218 ( $^{218}\text{U}_{126}$ ).

For the  $N = 8$  isotonic chain, the  $Z = 8$  (1p<sub>1=2</sub>) magic number is clearly seen from both the two- and the one-neutron separation energies, where the shell quantum number in the bracket is that of the shell closure. Both experimental data and our calculations also show a distinct sub-magic number at  $Z = 6$  (1p<sub>3=2</sub>). For the  $N = 20$  isotonic chain, besides the traditional  $Z = 8$  (1p<sub>1=2</sub>),  $Z = 20$  (1d<sub>3=2</sub>), and  $Z = 28$  (1f<sub>7=2</sub>) shell closures, a new (sub)shell closure (1d<sub>5=2</sub>) is clearly seen at  $Z = 14$ .  $^{34}\text{Si}_{20}$  has been recognized as a double magic nucleus by a previous shell-model calculation [34], due to a feature characteristic of double magic nuclei, i.e., it has a 0p 0h ground state and its two lowest excited states are intruders. For the  $N = 28$  isotonic chain, two neutron shell closures at  $Z = 20$  (1d<sub>3=2</sub>) and  $Z = 28$  (1f<sub>7=2</sub>) are reproduced quite well. For the  $N = 50$  isotonic chain, the agreement with available experimental data is very good. Although the  $Z = 28$  (1f<sub>7=2</sub>) and  $Z = 50$  (1g<sub>9=2</sub>) shell closures are still unaccessible experimentally up to now, they are clearly shown in our calculations. Based on the overall good agreement of the  $N = 50$  isotonic chain, we believe that our predictions are reliable.

For the  $N = 82$  isotonic chain, the  $Z = 50$  (1g<sub>9=2</sub>) shell closure is reproduced quite well while the  $Z = 82$  (1h<sub>11=2</sub>) shell closure is already in the unbound region. We note that there is a new (sub)shell closure (1g<sub>7=2</sub>) at  $Z = 58$  indicated in our calculations. It was argued long time ago that there is a whole "plateau" of stability for all the even  $58 \leq Z \leq 70$  nuclei in the  $N = 82$  isotonic chain [35, 36], i.e., the so-called "changing magicities". Our calculations do indicate this (sub)shell closure, supported also by the experimental data as shown in Fig. 2. However, the different deviation trends for nuclei with  $Z > 58$  and  $Z < 58$  indicate that some important features around  $Z = 58$  in the  $N = 82$  isotonic chain may be missed and/or misinterpreted in the relativistic mean field theory.

For the  $N = 126$  isotonic chain, immediately, we notice the seemingly big deviations of our calculations from the experimental data. From both the two- and the one-proton separation energies, we note that the experimental  $Z = 82$  (1h<sub>11=2</sub>) shell closure is underestimated somewhat by the relativistic mean field calculations. Our calculations also indicate another new (sub)shell closure (1h<sub>9=2</sub>) at  $Z = 92$  as what happened in Ref. [37], where  $^{218}\text{U}_{126}$  is studied as a double magic nucleus. We find that this is a unique phenomenon in the relativistic mean field theory while a large-scale shell-model calculation did not find this shell closure [38]. We also find that the use of other often used parameter sets in this region, such as NL3 [32] and NL-Z2 [33], does not change our conclusion.

The two-proton separation energy becomes negative when the nucleus becomes unstable with respect to two-proton emission. Hence, the two-proton drip-line nucleus for the corresponding isotonic chain is the one with two less protons than the nucleus at which  $S_{2p}$  first becomes negative. In the same way, we can also name the

one-proton drip-line nucleus. The predicted two- and one-proton drip-line nuclei based on our calculations are  $^{20}\text{M}_{98}$ ;  $^{46}\text{Fe}_{20}$ ,  $^{44}\text{C}_{20}$ ;  $^{58}\text{Zn}_{28}$ ,  $^{56}\text{Ni}_{28}$ ;  $^{100}\text{Sn}_{50}$ ;  $^{156}\text{W}_{82}$ ,  $^{152}\text{Y}_{82}$ ;  $^{220}\text{Pu}_{126}$ ,  $^{218}\text{U}_{126}$ , respectively. It is interesting to note that in some cases the two-proton drip-line nucleus and the one-proton drip-line nucleus are the same one, such as  $^{20}\text{M}_{98}$  in the  $N = 8$  isotonic chain and  $^{100}\text{Sn}_{50}$  in the  $N = 50$  isotonic chain. In other cases, the one-proton drip-line nucleus comes before the two-proton drip-line nucleus, which is easy to understand because the pairing interaction can increase the stability of even-even nuclei compared with its one-neutron less isotope. Depending on the pairing strength of the specific situation, the difference in neutron number between the two- and one-proton drip-line nucleus could be two or four. More specifically, the difference is 2 in the  $N = 20$ , 28 and 126 isotonic chains, while it is 4 in the  $N = 82$  isotonic chain.

## V. NUCLEAR RADII

The difference between neutron and proton root mean square (rms) radii,

$$R_{n(p)} = h r_{n(p)}^2 i^{1/2} = \frac{R_{n(p)} r^2 dr}{n(p) dr}^{1/2}; \quad (4)$$

where  $r_{n(p)}$  is the neutron (proton) density distribution, can be very large for nuclei with exotic isospin ratios, thus forms the so-called neutron (proton) skin [30], and even neutron (proton) halo [23, 24, 25]. The neutron rms radii (empty square) and proton rms radii (empty circle) of the  $N = 8, 20, 28, 50, 82$  and 126 isotonic chains are plotted in Fig. 3, where the experimental proton radii (solid circle with error bar) are extracted from the experimental charge radii [39] by the formula,

$$R_p^2 = R_c^2 - 0.64 \text{ fm}^2; \quad (5)$$

In Fig. 3, it is clearly seen that the agreement between our calculations and the experimental data is remarkably good. For  $^{37}\text{Cl}_{20}$  and  $^{50}\text{Ti}_{28}$ , the experimental data are somewhat larger than our theoretical predictions. Also, proton radii of two nuclei in the  $N = 126$  isotonic chain,  $^{208}\text{Pb}_{126}$  and  $^{209}\text{Bi}_{126}$ , seem to be a little bit overestimated in our calculations. Some kinks in Fig. 3 are due to sudden changes of deformations of the corresponding nuclei (see Fig. 4), including the one at  $Z = 16$  in the  $N = 28$  isotonic chain, the one at  $Z = 25$  in the  $N = 50$  isotonic chain, and the one at  $Z = 97$  in the  $N = 126$  isotonic chain. We would mention that the last few nuclei of each isotonic chain in Fig. 3 are unbound in our calculations with separation energies  $5 < S_{p(2p)} < 0$  MeV (see Fig. 2), thus the sudden increases of the proton radii do not necessarily imply appearances of proton halos.

One more thing we note is that unlike proton radii, which go up almost monotonously with increasing proton number, neutron radii usually go down first, then

go up slowly. This phenomenon is more obvious in the  $N = 8, 20, 28$ , and  $50$  isotonic chains. The reason behind this is not difficult to understand. Let us take the  $N = 8$  isotonic chain as an example. From  $Z = 2$  to  $Z = 6$ , the neutron radii decrease dramatically because these nuclei are neutron-rich nuclei where the continuum effects are very strong.  $^{11}_{\Lambda}Li$  is the first halo nucleus observed experimentally [24, 40]. The neutron radius becomes almost equal to the proton radius around  $Z = 8$ , then goes up very slowly with more protons added. Here, the reason is different from that for the neutron-rich side. In the proton-rich region, the neutrons are pulled outward somewhat by the attractive interaction between protons and neutrons.

## V I. DEFORMATIONS

Deformation is another important property of nuclei. It also could be used as one of the indicators of magicity conserving or losing features of the corresponding nucleus. In our previous work [20], we found that Sn isotopes are deformed in the neutron-rich region, which could be viewed as the magicity losing of proton magic number  $Z = 50$ . However, experimentally, it is difficult to obtain deformation knowledge of nuclei directly. One of the most usual methods is to extract deformation from the  $B(E2:0^+ \rightarrow 2^+)$  values by using the assumption of deformation [41]. Hence, all the nuclei have a finite deformation and also the analysis is limited to even-even nuclei. Due to this fact, we have to look at the extracted deformation with care. Most of the time, if the extracted deformation is small, the nucleus is expected to be spherical.

In Fig. 4, we plot the mass deformation parameters,  $\epsilon_2$ , for all the  $N = 8, 20, 28, 50, 82$ , and  $126$  isotonic chains as a function of proton number  $Z$ . The experimental data are extracted from the  $B(E2:0^+ \rightarrow 2^+)$  values given in Ref. [41]. The predictions of finite range droplet model (FRDM) are also shown for comparison [42]. From Fig. 4, it is easily seen that the agreement between our calculations and the results of FRDM model is remarkable. These two methods obtain essentially the same results for all the  $N = 20, 82$  and  $126$  isotones. For the  $N = 8$  isotonic chain, FRDM predicts  $^{18}_{10}Ne_8$ ,  $^{19}_{11}Na_8$ , and  $^{20}_{12}Mg_8$  to be slightly deformed, while in our calculations, these nuclei are spherical. For the  $N = 28$  isotonic chain, our calculations predict  $^{44}_{16}S_{28}$  to be deformed, which is consistent with both the experimental data and the predictions of the RHB method [43], while FRDM predicts it to be spherical. These two methods also differ in the predictions for the proton drip-line nuclei,  $^{63}_{35}Br_{28}$ ,  $^{64}_{36}Kr_{28}$ ,  $^{213}_{97}Bk_{126}$ , and  $^{214}_{98}Kr_{126}$ . We should note that these nuclei are already unstable against proton emission in our calculations (see Fig. 2). For the  $N = 50$  isotonic chain, the main differences between the predictions of these two methods exist in the region of  $20 < Z < 26$ . Our calculations show that these nuclei

are deformed, while FRDM predicts them to be nearly spherical.

Except for nuclei with  $Z < 18$  and  $Z > 30$  in the  $N = 28$  isotonic chain, and nuclei with  $20 < Z < 26$  in the  $N = 50$  isotonic chain, other nuclei in our calculations are more or less spherical. Although, at first sight, the agreement between our calculations (including the predictions of FRDM model) and the experimental data is not very good, we should keep in mind the limitations of the extracting method that we obtain the experimental deformation information. Within such a method, even the well-known spherical nuclei, such as  $^{16}_8O_8$  and  $^{40}_{20}Ca_{20}$ , are predicted to be deformed [41] (see Fig. 4). Therefore, the experimental data should be compared with caution. However, combined with other experimental knowledge, such as the reduced electric transition probability,  $B(E2)$ , and  $2_1^+$  energy, we can decide whether a nucleus is really deformed or not. The corresponding quantities for  $^{18}_{10}Ne_8$ ,  $^{32}_{12}Mg_{20}$ , and  $^{42}_{22}Ti_{20}$  are  $0.0269(26) e^2 b^2$ ,  $1887.3(2) \text{ keV}$ ;  $0.039(7) e^2 b^2$ ,  $885.5(7) \text{ keV}$ ;  $0.087(25) e^2 b^2$ ,  $1554.9(8) \text{ keV}$ ; respectively, which indicate these nuclei are really deformed [41]. The fact that our calculations did not find deformed configurations for these nuclei is probably due to the broken rotational symmetry in the relativistic mean field theory, which will be discussed below.

One of the long unsolved problems in the relativistic mean field theory is that it can not obtain deformed configurations for  $^{32}Mg$ , which is known to be strongly deformed experimentally [41], and other  $N = 20$  isotones around  $Z = 12$ , such as  $^{31}Na$  and  $^{30}Ne$  [30, 44]. However, the AMD method [17], the shell model calculations [34, 45], and the angular momentum projected generator coordinate method [46] can obtain a deformed configuration for  $^{32}Mg$ . In the shell model calculations [34, 45], it is demonstrated that the  $2p - 2h$  intruders dominate the ground states of  $^{30}Ne$ ,  $^{31}Na$ , and  $^{32}Mg$ , therefore lead to deformed ground states for these nuclei. While the studies of the AMD method and the angular momentum projected generator coordinate method clearly show that the zero-point energy associated with the restoration of the broken rotational symmetry [47] is indispensable for a correct description of the ground state of  $^{32}Mg$ .

As mentioned above, we have done the quadrupole constrained calculations for every nucleus in our present work in order to obtain its potential energy surface and find the ground state. Particularly in Fig. 5, we plot the potential energy surface of  $^{32}Mg$  as a function of deformation parameter  $\epsilon_2$ . Although very 'soft', an indication of a second minimum around  $\epsilon_2 = 0.5$  is clearly seen, which agrees well with unprojected AMD [17] and HFB [34] calculations. Therefore, we conclude that to obtain the deformed configuration for  $^{32}Mg$ , including  $^{18}Ne$  and  $^{44}Ti$ , the broken rotational symmetry in the relativistic mean field theory has to be restored. Since, so far, to our knowledge, such a calculation is still missing in the RMF method, no wonder no RMF calculations have succeeded in obtaining deformed configurations for these

nuclei. We also consider this as one motivation to introduce the angular momentum projection method into the present RMF model to restore the broken rotational symmetry as one of our next works.

In Ref. [12], the authors argued that their experimental high  $Q$  value,  $8344^{+165}_{-157}$  keV, for  $^{130}\text{Cd}$  is a direct signature of an  $N = 82$  shell quenching below  $^{132}\text{Sn}$ . While in our calculations, from the point of view of deformations, there is no indications of shell quenching for the whole  $N = 82$  isotonic chain, even in the neutron-rich side. In our calculations, the ground-state binding energy of  $^{130}\text{In}$ ,  $E = 1080.966$  MeV ( $\chi = 0.041$ ), together with the binding energy of  $^{130}\text{Cd}$ ,  $E = 1072.897$  MeV ( $\chi = 0.0$ ), give a  $Q$  of 8849 keV, which falls into the category of "quenched models" in Ref. [12]. Therefore, whether or not the  $N = 82$  shell is quenched in the neutron-rich region needs a more careful study both experimentally and theoretically.

## VII. CONCLUSIONS

Nuclei with magic numbers are very important in the study of nuclear physics, both theoretically and experimentally. The localized feature of "magic numbers" has received more and more attentions due to its importance to astrophysical problems and recent experimental developments to produce exotic nuclei in the laboratory. In the present work, we have adopted the relativistic mean field theory to study neutron magic nuclei with six classical magic numbers  $N = 8, 20, 28, 50, 82$ , and 126. The relativistic mean field theory that has proved to be very successful in describing many nuclear properties, due to its natural spin-orbit description and only a few parameters, is considered to be an ideal model to study not only stable nuclei but also exotic nuclei. In order to study all those nuclei in a proper way, we must take into account pairing correlations and deformation effects simultaneously. For nuclei with odd number of nucleons, the blocking effect must also be treated properly [48]. All these requirements make the calculation very complicated and time consuming, so up to now a systematic

study in the relativistic mean field theory including all these neutron magic numbers is still missing. However, due to the importance of these nuclei to various physical problems, such a study is in urgent need. This work is also part of our series of efforts to study magicity of magic numbers in the relativistic mean field theory.

In our systematic study of the neutron magic number isotonic chains, we have found a new proton magic number  $Z = 6$  in the  $N = 8$  isotonic chain. The shell closure feature at  $Z = 14$  in the  $N = 20$  isotonic chain is also reproduced very well. We have failed, however, to obtain deformed configurations for nuclei around  $Z = 12$  in the  $N = 20$  isotonic chain, which have been attributed to the broken rotational symmetry.  $N = 28$  has been predicted to lose its magicity in the proton-deient side of the isotonic chain, i.e., they are found to be deformed.  $N = 50$  seems to conserve its magicity in the proton-rich side while lose its magicity in the proton-deient side. This is in agreement with its proton counterpart,  $Z = 50$ , which is also found to lose its magicity in the neutron-rich side. For the  $N = 82$  isotonic chain, we have found that there is a (sub)shell closure at  $Z = 58$ , but the different deviation trends in the  $Z > 58$  and  $Z < 58$  region seem to imply that some features are missing and/or misinterpreted in the relativistic mean field theory. For the  $N = 126$  isotonic chain, both the two- and one-proton separation energies are a little bit overestimated. Our calculations also indicate a new (sub) shell closure at  $Z = 92$ . The total binding energies agree well with experiment around  $^{208}\text{Pb}$  and become larger than experiment with increasing proton number  $Z$ . The use of two other parameter sets, NL3 and NL-Z2, does not change the above conclusion. The predicted two-proton and one-proton drip-line nuclei for the  $N = 8, 20, 28, 50, 82$ , and 126 isotonic chains are  $^{20}_{12}\text{Mg}_8; {}^{46}_{26}\text{Fe}_{20}, {}^{44}_{24}\text{Cr}_{20}; {}^{58}_{30}\text{Zn}_{28}, {}^{56}_{28}\text{Ni}_{28}; {}^{100}_{50}\text{Sn}_{50}; {}^{156}_{74}\text{W}_{82}, {}^{152}_{70}\text{Yb}_{82}; {}^{220}_{94}\text{Pu}_{126}, {}^{218}_{92}\text{U}_{126}$ , respectively.

This work was partly supported by the Major State Basic Research Development Program Under Contract Number G2000077407 and the National Natural Science Foundation of China under Grant No. 10025522, 10221003 and 10047001.

---

[1] M. G. Mayer, *Phys. Rev.* 75, 1969 (1949).  
 [2] O. Haxel, H. H. D. Jensen, and H. E. Suess, *Phys. Rev.* 75, 1766 (1949).  
 [3] E. M. Burbidge, G. R. Burbidge, W. A. Fowler, and F. Hoyle, *Rev. Mod. Phys.* 29, 547 (1957).  
 [4] A. Bohr and B. M. Ottelson, *Nuclear Structure* (New York, Benjamin, 1969).  
 [5] P. Ring and P. Schuck, *The Nuclear Many-Body Problem* (Springer, New York, 1980).  
 [6] K. Heyde, *Basic Ideas and Concepts in Nuclear Physics* (IO, Bristol, 1999).  
 [7] J. D. Walecka, *Ann. Phys. (N.Y.)* 83, 491 (1974).  
 [8] B. D. Serot and J. D. Walecka, *Adv. Nucl. Phys.* 16, 1 (1986).  
 [9] P. G. Reinhard, *Rep. Prog. Phys.* 52, 439 (1989).  
 [10] D. Hirata, H. Toki, T. Watabe, I. Tanigata, and B. V. Carlson, *Phys. Rev. C* 44, 1467 (1991).  
 [11] P. Ring, *Prog. Part. Nucl. Phys.* 37, 193 (1996).  
 [12] I. Dillmann et al., *Phys. Rev. Lett.* 91, 162503 (2003).  
 [13] A. Ozawa et al., *Phys. Rev. Lett.* 84, 5493 (2000).  
 [14] K. L. Kratz, J. P. B. Bouchez, F. K. Thielemann, P. Moeller, and B. Pfeiffer, *Astrophys. J.* 403, 216 (1993).  
 [15] R. C. Nayak, *Phys. Rev. C* 60, 064305 (1999).  
 [16] C. Samanta and S. Adhikari, *Phys. Rev. C* 65, 037301 (2002).  
 [17] Masaaki Kimura and Hisashi Horiuchi, *Prog. Theor.*

Phys. 107, 33 (2002).

[18] B. C. Chen, J. D. obaczewski, K. -L. K. ratz, K. Langanke, B. Pfeifer, F. -K. Thielmann, and P. Vogel, Phys. Lett. B 355, 37 (1995).

[19] J. Meng, I. Tanihata, and S. Yamaji, Phys. Lett. B 419, 1 (1998).

[20] L. S. Geng, H. Toki, and J. Meng, arXiv:nucl-th/0312027.

[21] L. S. Geng, H. Toki, S. Sugimoto, and J. Meng, Prog. Theor. Phys. 110, 921 (2003).

[22] H. L. Yadav, S. Sugimoto, and H. Toki, Mod. Phys. Lett. A 17, 2523 (2002).

[23] N. Sandulescu, L. S. Geng, H. Toki, and G. H. Hillhouse, Phys. Rev. C 68, 054323 (2003).

[24] J. Meng, Nucl. Phys. A 635, 3 (1998); J. Meng and P. Ring, Phys. Rev. Lett. 77, 3963 (1996).

[25] J. Meng and P. Ring, Phys. Rev. Lett. 80, 460 (1998).

[26] N. Sandulescu, Nguyen Van Giai, and R. J. Liotta, Phys. Rev. C 61, 061301(R) (2000).

[27] Y. Sugahara and H. Toki, Nucl. Phys. A 579, 557 (1994); Y. Sugahara, Ph.D. thesis, Tokyo Metropolitan University, 1995.

[28] Y. K. Gambhir, P. Ring, and A. Thimet, Ann. Phys. (N.Y.) 194, 132 (1990).

[29] H. Flocard et al., Nucl. Phys. A 203, 433 (1973).

[30] L. S. Geng, H. Toki, A. O. zawa, and J. Meng, Nucl. Phys. A 730, 80 (2004).

[31] G. Audi and A. H. Wapstra, Nucl. Phys. A 595, 409 (1995).

[32] G. A. Lalazissis, J. Konig, and P. Ring, Phys. Rev. C 55, 540 (1997).

[33] M. Bender, K. Rutz, P.-G. Reinhard, J. A. Maruhn, and W. Greiner, Phys. Rev. C 60, 034304 (1999).

[34] E. Caurier, F. Nowacki, A. Poves, and J. Retamosa, Phys. Rev. C 58, 2033 (1998).

[35] A. Abbas, Phys. Rev. C 29, 1033 (1984).

[36] P. Arumugam, S. K. Patra, and A. Abbas, arXiv:nucl-th/0309034.

[37] K. Rutz, M. Bender, P.-G. Reinhard, J. A. Maruhn, and W. Greiner, Nucl. Phys. A 634, 67 (1998).

[38] E. Caurier, M. Reinhard, and H. Grawe, Phys. Rev. C 67, 054310 (2003).

[39] H. De Vries, C. W. De Jager, and C. De Vries, At. Data Nucl. Data Tables 36, 495 (1987).

[40] I. Tanihata et al., Phys. Rev. Lett. 55, 2676 (1985).

[41] S. Ramam, C. W. Nestor, Jr., and P. Tikkkanen, At. Data Nucl. Data Tables 78, 1 (2001).

[42] P. Moller, J. R. Nix, and W. D. Meyer, At. Data Nucl. Data Tables 59, 1 (1995).

[43] G. A. Lalazissis, D. Vretenar, P. Ring, M. Stoitsov, and L. M. Robledo, Phys. Rev. C 60, 014310 (1999).

[44] G. A. Lalazissis, D. Vretenar, and P. Ring, nucl-th/0109027; G. A. Lalazissis and S. Ramam, At. Data Nucl. Data Tables 71, 40 (1999).

[45] Yutaka Utsuno, Takaharu Otsuka, Takahiro Mizusaki, and Michio Honnma, Phys. Rev. C 60, 054315 (1999).

[46] R. R. Rodriguez-Guzman, J. L. Ejido, and L. M. Robledo, Phys. Rev. C 62, 054319 (2000); Phys. Lett. B 474, 15 (2000).

[47] P.-G. Reinhard et al., Phys. Rev. C 60, 014316 (1999).

[48] L. S. Geng, H. Toki, and J. Meng, Phys. Rev. C 68 061303(R) (2003).

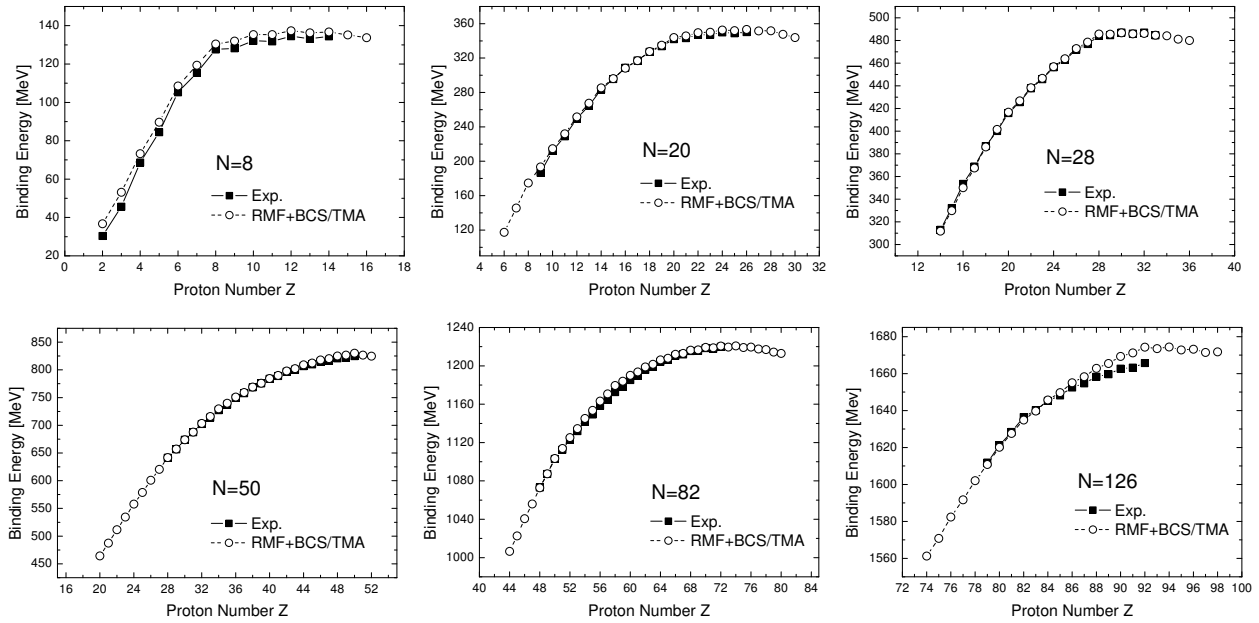


FIG. 1: The binding energies of the  $N = 8, 20, 28, 50, 82$ , and  $126$  isotonic chains as a function of the proton number  $Z$ . The results obtained from the deformed RMF+BCS calculations with the TMA set (open circle) are compared with available experimental data including extrapolated data (solid square) [31].

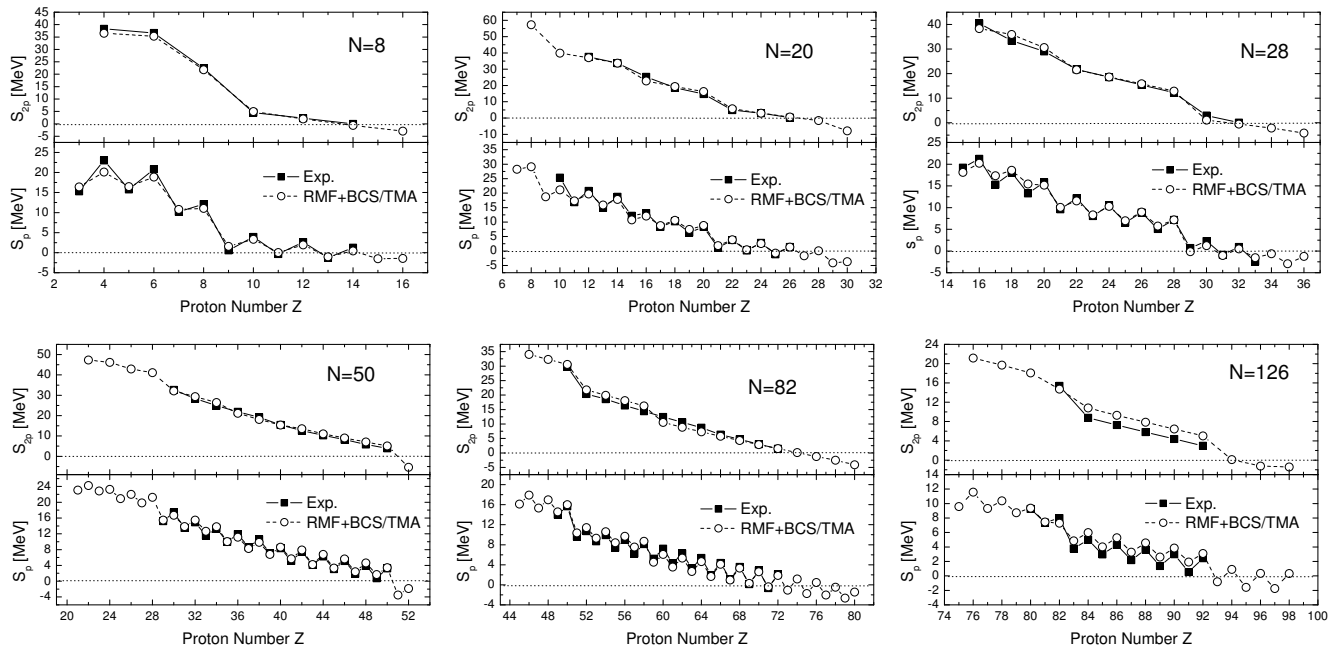


FIG. 2: The two- and one-proton separation energies,  $S_{2p}$  and  $S_p$ , of the  $N = 8, 20, 28, 50, 82$ , and  $126$  isotonic chains as a function of the proton number  $Z$ . The results obtained from the deformed RMF+BCS calculations with the TMA set (open circle) are compared with available experimental data including extrapolated data (solid square) [31].

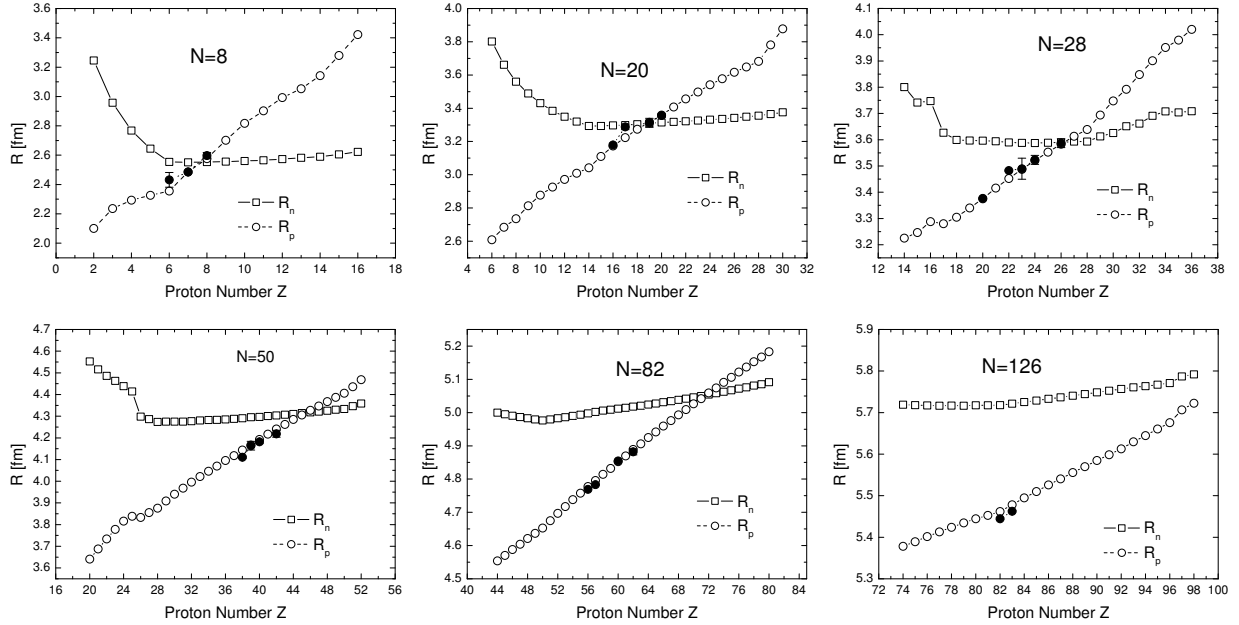


FIG. 3: The rms neutron radii,  $R_n$ , and proton radii,  $R_p$ , of the  $N = 8, 20, 28, 50, 82$ , and  $126$  isotonic chains as a function of the proton number  $Z$ . The results obtained from the deformed RMF+BCS calculations with the TM A set (open circle) are compared with available experimental data [39] (solid square with error bar).

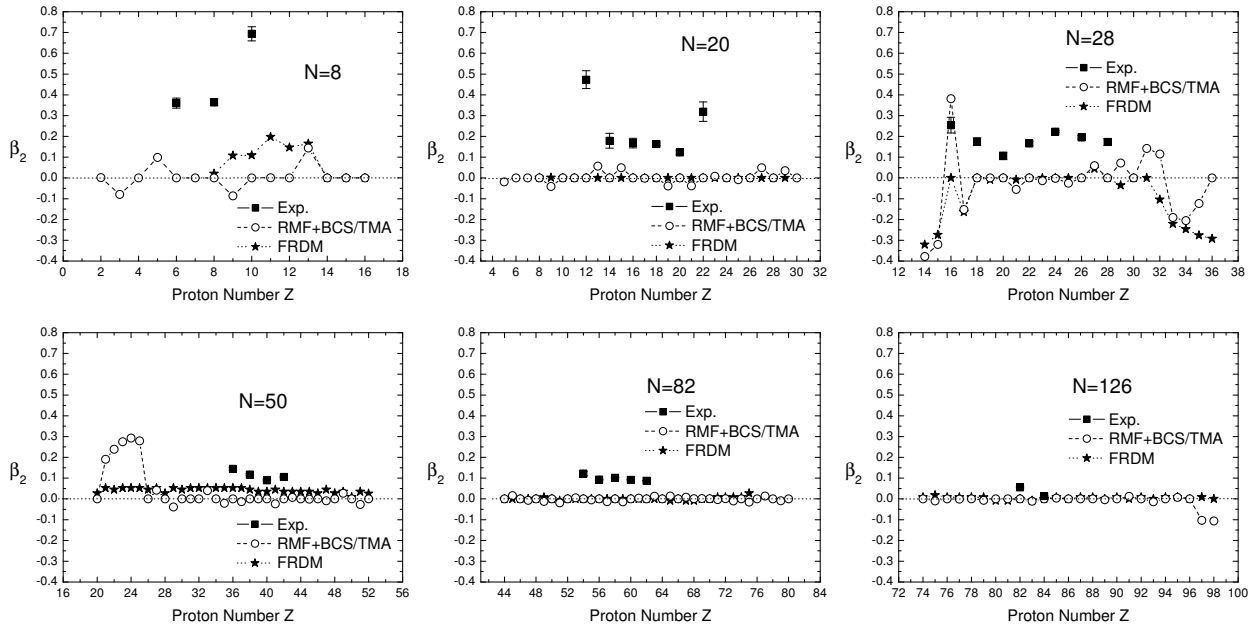


FIG. 4: The mass quadrupole deformation parameters,  $\beta_2$ , of the  $N = 8, 20, 28, 50, 82$ , and  $126$  isotonic chains as a function of the proton number  $Z$ . The results obtained from the deformed RMF+BCS calculations with the TM A set (open circle) are compared with the predictions of FRDM model (solid star) [42], and available experimental data (solid square) extracted from the  $B(E2:0^+ \rightarrow 2^+)$  values [41]. We note that the extracted deformation does not mean that the corresponding nucleus is really deformed.

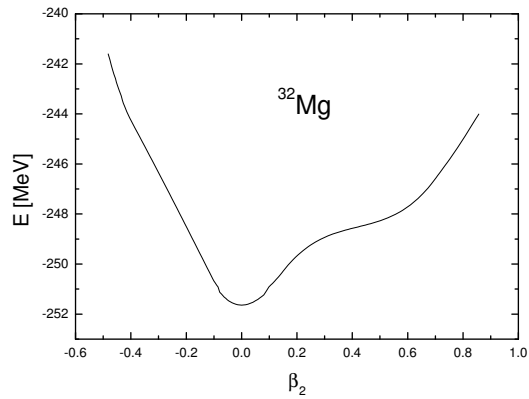


FIG. 5: The potential energy surface of  $^{32}\text{Mg}$  as a function of deformation parameter  $\beta_2$ .